

Calculation of the Magnetostatic Energy in Spin Density Functional Theory

Lórien MacEnulty^{1, 2, a)} and David D. O'Regan^{1, b)}

¹*School of Physics, AMBER and CRANN, Trinity College Dublin, The University of Dublin, Dublin 2, Ireland*

²*Department of Physics and Astronomy, Drake University, Harvey-Ingham Hall,
2804 Forest Avenue, Des Moines, Iowa 50311, USA*

^{a)} Corresponding author: lorien.macenuity@drake.edu

^{b)} david.o.regan@tcd.ie

Abstract. In density functional theory calculations of materials and molecules, it is conventional to neglect the relativistic magnetostatic contribution of unpaired electron spins to the total energy and potential. For small systems, the magnetostatic contribution to the total energy is negligible, yet it is not obvious that it remains negligible in extended systems with high spin magnetic moment. We make use of a mathematical shortcut, using a fictitious magnetic charge density, to calculate the magnetic field and to determine the degree to which this relativistic effect can be ignored in electronic structure calculations. Using this, we compare the strength of the magnetostatic energy to the electrostatic energy. This ratio is consistently on the order of 10^{-5} , which is on the order of $1/c^2$ in atomic units, as is expected from its formula.

INTRODUCTION

Electron Spin, Magnetization, and Density Functional Theory

Quantum effects give rise to an intrinsic angular momentum or spin, characteristic of all particles, which interacts with external magnetic fields. For collinear spins, unpaired electrons in valence orbitals of atoms contribute to the overall magnetization \vec{M} via linear accumulation of the z-component of their spin-generated magnetic moments:

$$\vec{M} = \frac{-\mu_B}{e} (\rho^\uparrow - \rho^\downarrow) \hat{M}. \quad (1)$$

Here, ρ^σ is the charge density of electrons of spin σ , $\mu_B = 1/2$ in atomic units is the Bohr magneton, e is the electronic charge, and \hat{M} is the magnetization orientation unit vector.

Density functional theory (DFT), a computational method for calculating quantum properties, allows us to solve the many-body Schrödinger equation indirectly by asserting that the energy may be written as a function of the electron probability density, a function of spatial coordinates.² The Kohn-Sham equation, an auxiliary DFT analog to the Schrödinger equation, can incorporate both quantum interactions and relativistic interactions. We are concerned with the latter axis, wherein any relativistic electron-spin-generated magnetostatic energy is considered a higher order relativistic correction to the electrostatic Hartree term. Usually, this term is negligible, although it is known to play a role in determining magnetic domain sizes. The effects and energy scales that typically compete with the magnetostatic energy are the spin-orbit energy and the exchange-correlation magnetic field energy. In systems with high spin magnetic moment, such as in elemental manganese, the term's negligibility is not immediately evident.

The magnetostatic energy term manifests in the many-body electronic Hamiltonian. In this context, we can begin to approximate this corrective term in Kohn-Sham DFT, including relativistic exchange and correlation effects. In our own work, we explore the non-self-consistent energy contribution of this term to the density, not the self-consistent effect. Nonetheless, it is worth recalling the weakly relativistic Hamiltonian for a vanishing applied magnetic field,³

$$\hat{H} = \hat{T} + \int d^3r [\hat{n}(\vec{r})V_{\text{ext}}(\vec{r})] + \int d^3r \int d^3r' \left[\frac{e^2}{2} \frac{\hat{n}(\vec{r})\hat{n}(\vec{r}')}{|\vec{r}-\vec{r}'|} - 2\pi\mu_B^2 \hat{m}^i(\vec{r}) \left(\frac{2}{3} \delta_{ij} \delta(\vec{r}-\vec{r}') + d_{ij}(\vec{r}-\vec{r}') \right) \hat{m}^j(\vec{r}') \right], \quad (2)$$

where \hat{T} is the kinetic energy operator, $\vec{r} - \vec{r}'$ is the source-field displacement, and $\hat{m}(\vec{r})$ is the magnetization density operator. The tensor d_{ij} is defined as³

$$d_{ij}(\vec{r} - \vec{r}') = -\frac{1}{4\pi} \nabla_i \nabla'_j \frac{1}{|\vec{r} - \vec{r}'|} + \frac{1}{3} \delta_{ij} \delta(\vec{r} - \vec{r}'). \quad (3)$$

For the purposes of this investigation, we are primarily interested in the μ_B^2 term of Eq. (2) but refer the reader to Refs. 3 and 4 for further clarification on the constituents of the previous Hamiltonian.

METHODS

A versatile algorithm was built to systematically determine the magnetostatic energy contribution U_M of valence electron spin given a static magnetization \vec{M} . The systems with which we are concerned have no free current density. We thus derive the curl of the magnetic field strength \vec{H} to be zero, so effectively, \vec{H} may be written as the negative gradient of a scalar potential, which we will call the scalar magnetic potential ϕ_M . To obtain this ϕ_M , we start by finding the fictitious magnetic charge density ρ_M , an exclusively mathematical object simulating the north and south poles of magnetic bodies, defined as

$$\rho_M = -\nabla \cdot \vec{M}. \quad (4)$$

We then extract a density table as a function of coordinates. The Fast Fourier Transform method translates the density table into reciprocal space. We construct the reciprocal potential $\widetilde{\phi}_M(\vec{k})$ by dividing terms in the reciprocal density table by the inverse k^2 , thereby employing the Fourier space equivalent of Poisson's equation for magnetism:⁵

$$\widetilde{\phi}_M(\vec{k}) = \frac{\widetilde{\rho}_M(\vec{k})}{k^2}. \quad (5)$$

It is expected that $\widetilde{\rho}_M$ averages to zero inside the cell in source-free magnetism, so the limit of $\widetilde{\phi}_M(\vec{k})$ as $k \rightarrow 0$ is separately set to zero in the program. The Inverse Fourier transform of the reciprocal potential table yields ϕ_M , and thus we attain $\vec{H} = -\nabla \phi_M$. The magnetostatic energy U_M is then obtained via the volume integral in Eq. (6), which is preceded by $\mu_0 = 4\pi\alpha^2$ in atomic units, where $\alpha = \frac{1}{c} \approx \frac{1}{137}$ is the fine structure constant:⁶

$$U_M = \int_V \frac{\mu_0}{2} (M^2 + \vec{H} \cdot \vec{M}) dV. \quad (6)$$

We applied the algorithm to a variety of atomic systems modeled by both theoretically and computationally derived

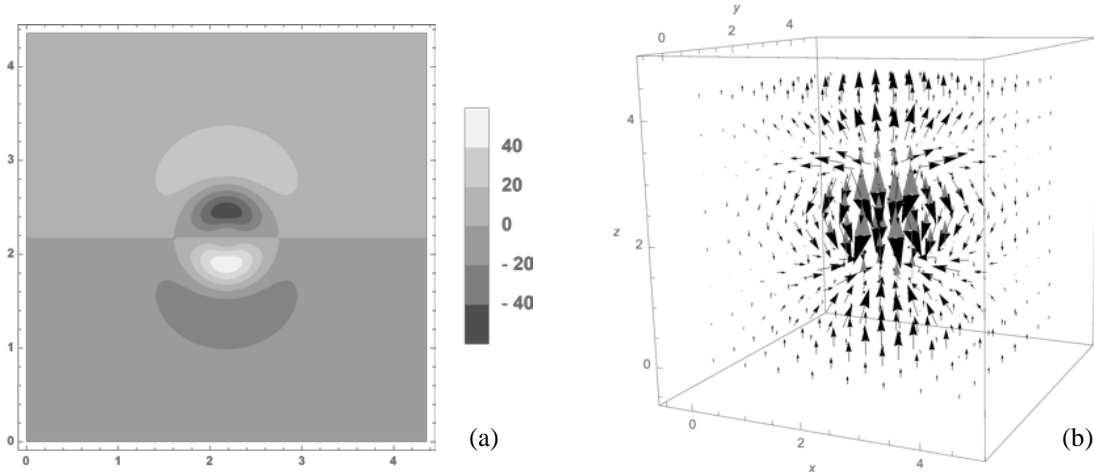


FIGURE 1. (a) Magnetic charge density ρ_M in a.u. of Mn 3d orbital resultant of magnetization pointing in z-direction (x - z plane, $y = \frac{a}{2} a_0$). (b) Vector field of magnetization \vec{M} (gray) and magnetic field strength \vec{H} (black) of Mn 3d orbital. Values in a.u.

electron densities and enclosed in various crystal lattices. One model system investigated comprised a single manganese atom, the elemental transition metal with the highest spin magnetic moment, at the center of a cube of lattice constant $4.35 a_0$. Assuming the spin is collinear, Mn adopts a total magnetic moment along the quantization axis \hat{z} of $5 \mu_B$ due to its five unpaired electrons in the 3d valence shell. The magnetization under consideration, of similar form to Eq. (1), is thus

$$\vec{M}_{\text{Mn}}(r) = \frac{5}{2} \left[\frac{4}{27\sqrt{10}} \left(\frac{Z_{\text{eff}}}{3a_0} \right)^{\frac{3}{2}} \left(\frac{r \cdot Z_{\text{eff}}}{a_0} \right)^2 \exp \left[\frac{-r \cdot Z_{\text{eff}}}{3a_0} \right] \right]^2 \hat{z}, \quad (7)$$

where r is the distance from the origin, set at (0,0,0), and Z_{eff} is the effective nuclear charge of Mn.

RESULTS AND DISCUSSION

Figure 1(a) shows the magnetic charge density generated by a single, highly idealized Mn atom at the center of a cube. As expected, we observe regions of opposite sign corresponding to the south and north poles of the magnetization field. Figure 1(b) is a three-dimensional vector field plot of both \vec{M} and \vec{H} as functions of Cartesian coordinates. The flux of \vec{H} appears to oppose that of \vec{M} amidst the approximate domain of the Mn $3d$ orbital. This is precisely the behavior we expect to see mathematically and provides a degree of validation that the algorithm works as expected. The magnetostatic energy was converged as a function of increasing interpolation order and number of points.

The magnetostatic energy of this system converges to a value of around -0.0220 a.u. per atom. Across all systems, it is exclusively the energy contribution of the $\vec{H} \cdot \vec{M}$ term, denoted $U_{\vec{H} \cdot \vec{M}}$, that varies with orientation, whereas the \vec{M}^2 volume integral remains constant. By contrast, the electrostatic energy of the same atomic system is approximately 609 a.u. per atom. The ratio of magnitudes of magnetostatic to electrostatic energy contributions is consistently on the order of 10^{-5} across the various atomic systems tested, including the cubic system and an FCC lattice system (both primitive and conventional unit cells, lattice constant $4.35 \sqrt{2} a_0$). This ratio is physically plausible since the magnetostatic term is scaled by a factor of μ_0 , which is proportional to the square of the fine structure constant.

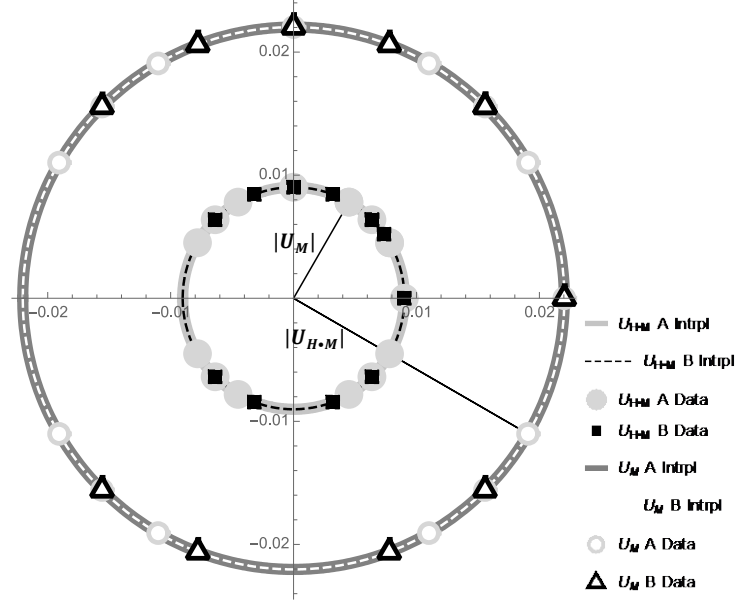


FIGURE 2. Magnetostatic energy in a.u. of single Mn atom cubic system as a function of \vec{M} orientation. Distance from the origin to the point is $|U_M|$ or $|U_{\vec{H} \cdot \vec{M}}|$ (see legend). Legend entries denoted “A” signify \vec{M} orientation in the x-y plane ($M_z = 0$); those denoted “B” are beholden to the plane generated by vectors $\{0,0,1\}$ and $\{1,1,1\}$. “Intrpl” = interpolated function of circle.

This cubic system was then immersed in a crystalline lattice environment and subjected to computational testing for an expected magnetostatic anisotropy. The orientation of \vec{M} was varied in order to measure its effect on the magnitude of the magnetostatic energy. In crystalline lattice environments, the distance between atoms along a given vector is not generally the same, and thus variation of the dipole orientation would enlighten us to the existence of a discernible anisotropy contribution.¹ As demonstrated in Fig. 2 and validated across multiple other orientations of \vec{M} , the cubic system in question exhibits a subtle, even negligible energy variation with orientation angle; the magnitude

of \mathbf{U}_M remains close to constant despite the change in orientation of $\overline{\mathbf{M}}$.

CONCLUSIONS

The spin-generated magnetostatic contribution to the total energy of atomic systems is small, consistently on the order of $1/c^2$ times its electrostatic counterpart. We cannot conclude definitively that DFT practitioners may exclude the magnetostatic dipole energy, noting, however, that we did not investigate a situation in which the dipole and spin-exchange-correlation magnetic field energies compete. This approach demonstrates the value of the magnetic charge density as an interesting stratagem for computing the properties of magnetic fields. We hope to inspire further investigation of the magnetic charge density in the context of approximate functional construction for relativistic DFT, where it may be useful for the study of systems with less localized spin densities or embedded in inherently anisotropic crystal structures.

ACKNOWLEDGMENTS

This educational research experience was enabled by the Science Foundation Ireland (SFI) through the Advanced Materials and Bioengineering Research Centre (AMBER, Grant No. 12/RC/2278). Many thanks to Okan K. Orhan.

REFERENCES

- [1] J. Coey, *Magnetism and Magnetic Materials* (Cambridge University Press, Cambridge, England, 2010), p. 66, 168.
- [2] C. Fiolhais, F. Nogueira, and M. Marques, *A Primer in Density Functional Theory*, edited by C. Fiolhais, F. Nogueira, and M. A. L. Marques, Lecture Notes in Physics Vol. 620 (Springer Verlag, Berlin, Heidelberg, 2003), pp. 1–5.
- [3] C. Pellegrini, T. Müller, J. K. Dewhurst, S. Sharma, A. Sanna, and E. K. U. Gross, *Phys. Rev. B* **101**, 144401 (2020).
- [4] H. J. F. Jansen, *Phys. Rev. B* **38**, 8022 (1988).
- [5] J. Mathews and R. Walker, *Mathematical Methods in Physics*, 2nd ed. (Addison-Wesley Publishing Co., Menlo Park, CA, 1970), pp. 239–245.
- [6] D. Griffiths, *Introduction to Electrodynamics*, 4th ed. (Pearson, New York, 2017), p. 330.